

Supporting Information

Efficient Inverted Perovskite Solar Cells With Low-Temperature Processed NiOx/SAM Hole Transport Layer

Yi Guo,^{ab} Like Huang*,^b Chaofeng Wang,^b Shuang Liu,^b Jiajia Huang,^b Xiaohui Liu,^b
Jing Zhang,^b Ziyang Hu,^b Yuejin Zhu*^a

a. School of Information Engineering, College of Science and Technology, Ningbo University, Ningbo 315300, China

b. Department of Microelectronic Science and Engineering School of Physical Science and Technology, Ningbo University, Fenghua Road 818, Ningbo 315211, China

L. Huang

National Laboratory of Solid State Microstructures, Nanjing University, Nanjing 210093, China

Y. Zhu

School of Information Engineering, College of Science and Technology, Ningbo University, Ningbo 315300, China

**Corresponding authors.*

L. Huang, Y. Zhu

E-mail addresses: huanglike@nbu.edu.cn (L. Huang); zhuyuejin@nbu.edu.cn (Y. Zhu).

1. Experimental Section

1.1 Material

Laser etched ITO ($1.5 \times 1.5 \text{ cm}^2$, $7 \Omega \text{ sq}^{-1}$) glass substrates, [6,6]-phenyl-C61-butyric acid methyl ester (PC₆₁BM, 99%) were purchased from Advanced Election Technology Co. Ltd., China. Lead iodide (PbI₂, 99.99%), lead bromide (PbBr₂, 99.99%), cesium iodide (CsI, 99.99%), formamidine hydroiodide (FAI, 99.5%), methylammonium iodide (MAI, 99.5%), bathocuproine (BCP, 99.9%) and [2-(3,6-dimethoxy-9H-carbazol-9-yl)ethyl]phosphonic acid (MeO-2PACz, 98%) were purchased from Xi'an Polymer Light Technology Corp. Anhydrous ethanol (99.5%) were purchased from Macklin. The N,N-dimethylformamide (DMF, 99.8%), Dimethylsulfoxide (DMSO, 99.8%), chlorobenzene (CB, 99.9%) and Isopropanol (IPA, 99.5%) were purchased from Aladdin.

1.2 Device fabrication

The glass/ITO substrates were cleaned by deionized water and ethanol, respectively, in an ultrasonic bath at $\sim 25 \text{ }^\circ\text{C}$ for 15 minutes, and then blow dry the substrates. Then, the dry substrates were treated with UV-ozone for 15 min to remove any chemical residuals and enhance the surface wettability of the ITO substrates. The synthesis of nickel oxide nanoparticles (NiO_x NPs) follows our previous works.¹ The as-prepared NiO_x solution with 15 mg/mL in deionized water was spin-coated onto the ITO substrates at 3000 rpm for 30 s, and the substrate was subsequently annealed at $120 \text{ }^\circ\text{C}$ for 10 min in ambient air. The MeO-2PACz molecules with 1 mg/mL in anhydrous ethanol (dispersed by ultrasonic bath for ~ 10 minutes) were spin-coated at 3000 rpm for 30 s, and annealed at $100 \text{ }^\circ\text{C}$ for 10 min in the glove box. 1.4 M perovskite precursor solution was prepared by mixing FAI, MAI, CsI, PbBr₂, PbI₂ in DMF and DMSO (4:1/v:v) with a chemical formula of Cs_{0.05}(FA_{0.92}MA_{0.08})_{0.95}Pb(I_{0.9}Br_{0.1})₃. 40 μL of perovskite solution was spin-coated on different substrates at 1000 rpm for 10 s and 5000 rpm for 30 s. Then, 180 μL of anti-solvent CB was dropped quickly at 10 s before

the end of spin-coating. After cooling, PCBM solution with 20 mg/mL in CB was spin-coating at 3000 rpm for 30 s. Subsequently, the upper clear liquid of BCP supersaturated solution was dripped onto the PCBM film via drop by drop at 5500rpm for 30 s, and then annealed at 70 °C for 5 min. Finally, the device was completed by the thermal deposition of ~60 nm thick Ag back electrode under high vacuum ($<3\times 10^{-4}$ Pa).

2. Device Characterization

The current density-voltage ($J-V$) curves, conductivity measurement and the space-charge-limited current (SCLC) were measured by a Keithley 4200 source meter unit under an AM 1.5G solar (100 mW/cm²), the active area was 0.04 cm² (Newport, 91192A). The surface potential and roughness of the films were measured by atomic force microscopy (AFM) of Dimension 3100V (SPM, Veeco, USA). The surface morphology of the perovskite film was obtained by scanning electron microscope (Hitachi, SU-70, Japan). X-ray diffraction patterns (XRD) were collected by using a Bruker instrument using Cu K α radiation at scan rate of 4°min⁻¹ (D8 advance, Germany). The element composition and orbital binding energy of elements were tested by X-ray photoelectron spectroscopy (XPS, Thermo Scientific K-Alpha). The surface work function (WF) and energy level position of the thin film are obtained via ultraviolet photoelectron spectroscopy (UPS, Thermo Fisher Nexsa with the He I (21.22 eV) emission line). The absorption spectra and transmission spectra of films on substrates were measured by UV-vis spectrophotometer (Agilent Cary 5000, USA). The external quantum efficiency (EQE) of the device was tested via a Newport EQE system in the wavelength range of 300–900 nm. The steady-state fluorescence (PL) spectra and the time-resolved photoluminescence (TRPL) spectra of the PVK films on different substrates were tested by fluorescence spectrophotometer (Agilent, USA), PL spectrometer (Horiba, Japan), respectively. The transient photocurrent (TPC) decay, transient photovoltage (TPV) decay, electrochemical impedance spectroscopy (EIS) and

Mott–Schottky characteristics were conducted on electrochemical workstation (Zahner, Germany).

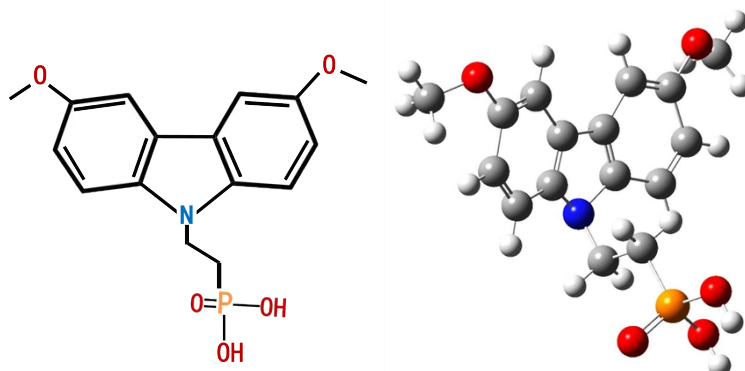


Fig. S1 Molecular structure of MeO-2PACz.

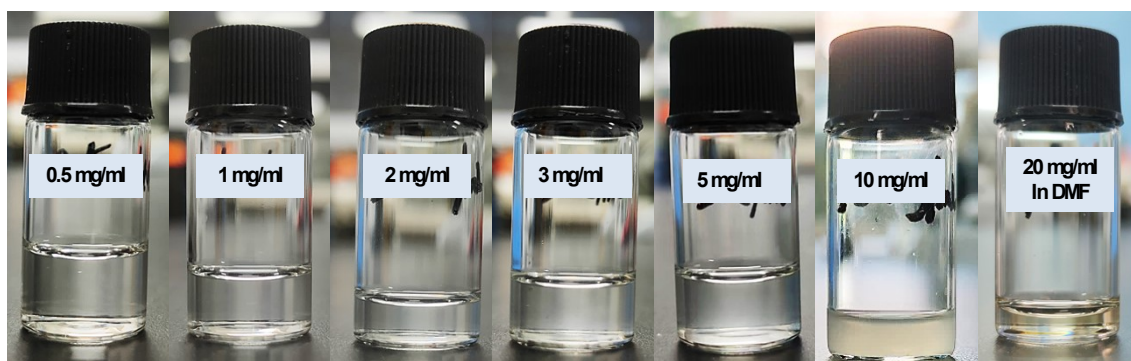


Fig. S2 Solution of self-assembled molecules (MeO-2PACz) in anhydrous ethanol and DMF.

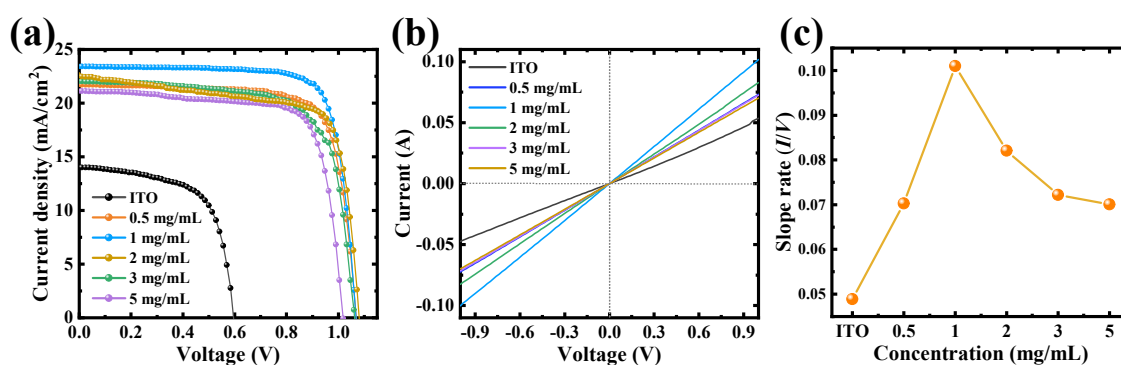


Fig. S3 (a) J - V curves for devices with different concentrations of MeO-2PACz (0.5~5 mg/mL) modified ITO. (b) The I - V curves for evaluating the conductivity of different substrates and (c) their slope (I/V) variation with concentration.

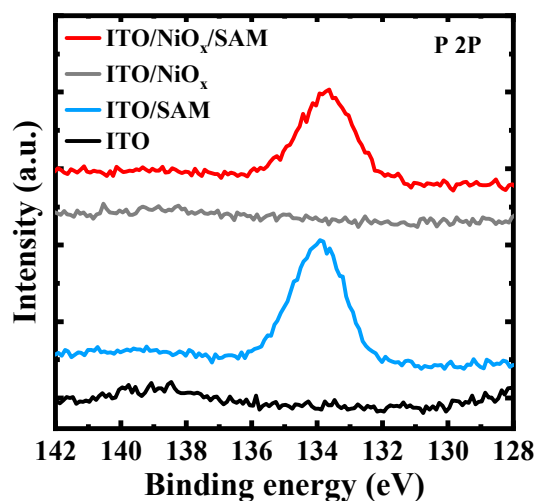


Fig. S4 X-ray photoelectron spectroscopy (XPS) at the P 2p region of ITO and ITO/NiO_x before and after adsorption of MeO-2PACz (1 mg/mL).

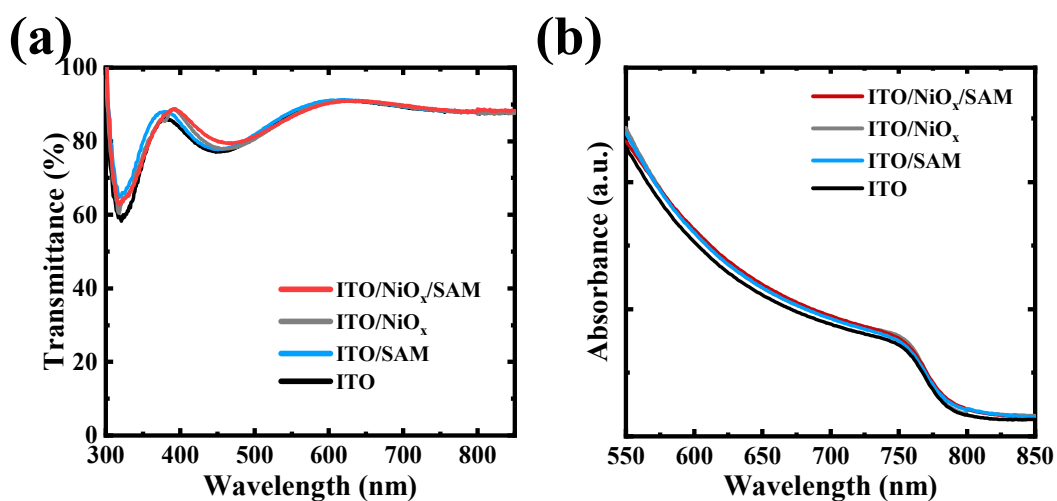


Fig. S5 (a) The transmittance of ITO, ITO/SAM, ITO/NiO_x, ITO/NiO_x/SAM. (b) UV-visible absorption spectra of the perovskite films deposited on different substrates. The ITO or NiO_x substrates were modified by MeO-2PACz with 1 mg/mL in anhydrous ethanol.

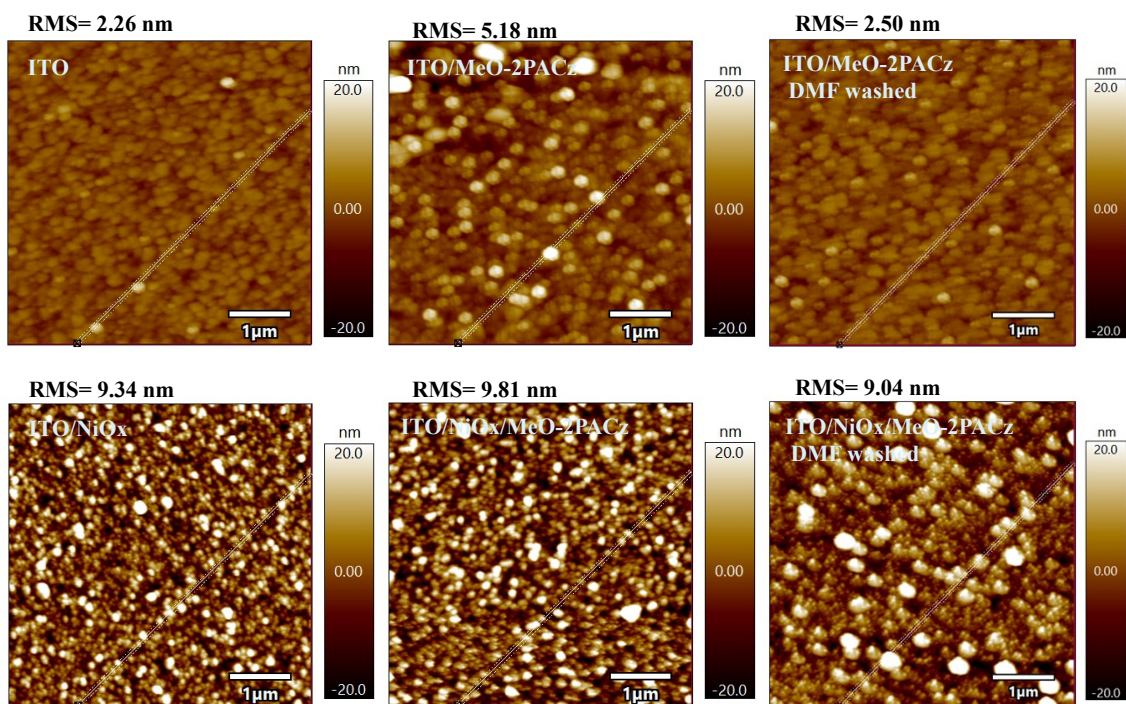


Fig. S6 The AFM morphology and roughness of substrates with different treatments.

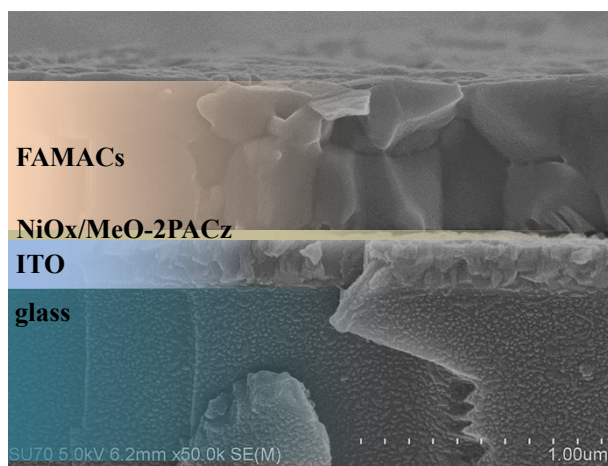


Fig. S7 Cross-sectional SEM images of perovskite film on ITO/NiO_x/SAM.

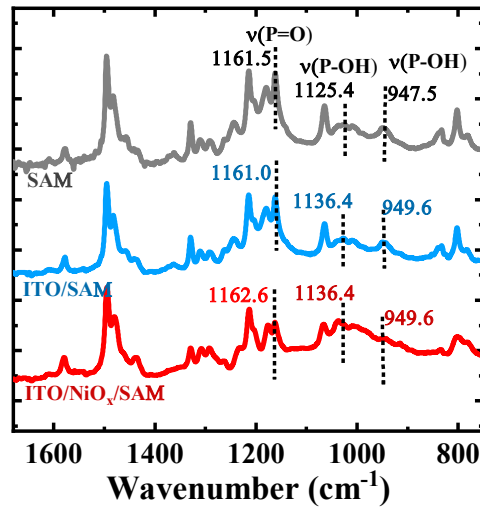


Fig. S8 The FTIR spectrum of bulk MeO-2PACz (grey) and the RAIRS of MeO-2PACz adsorbed on ITO (blue) and ITO/NiO_x (red).

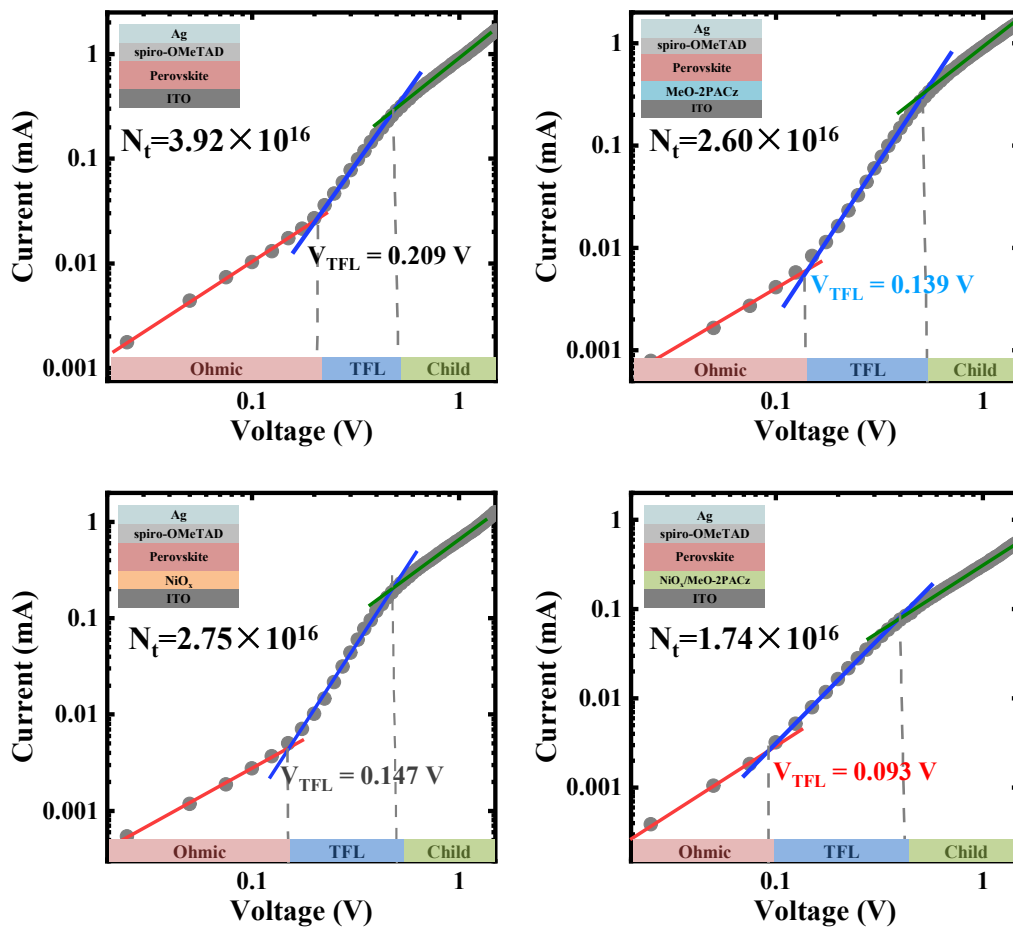


Fig. S9 Dark *I-V* curves of the “hole-only” devices with perovskite film on different substrates. Insets showed the device architectures.

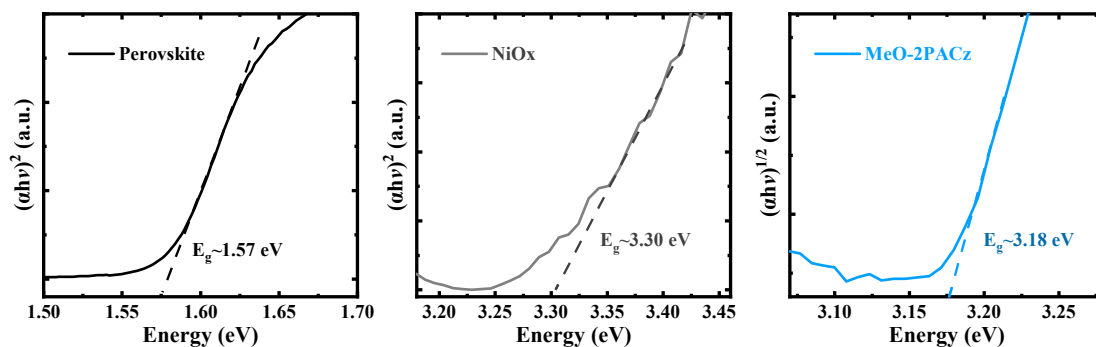


Fig. S10 The UV-Vis absorbance spectra of perovskite, NiO_x, and MeO-2PACz.

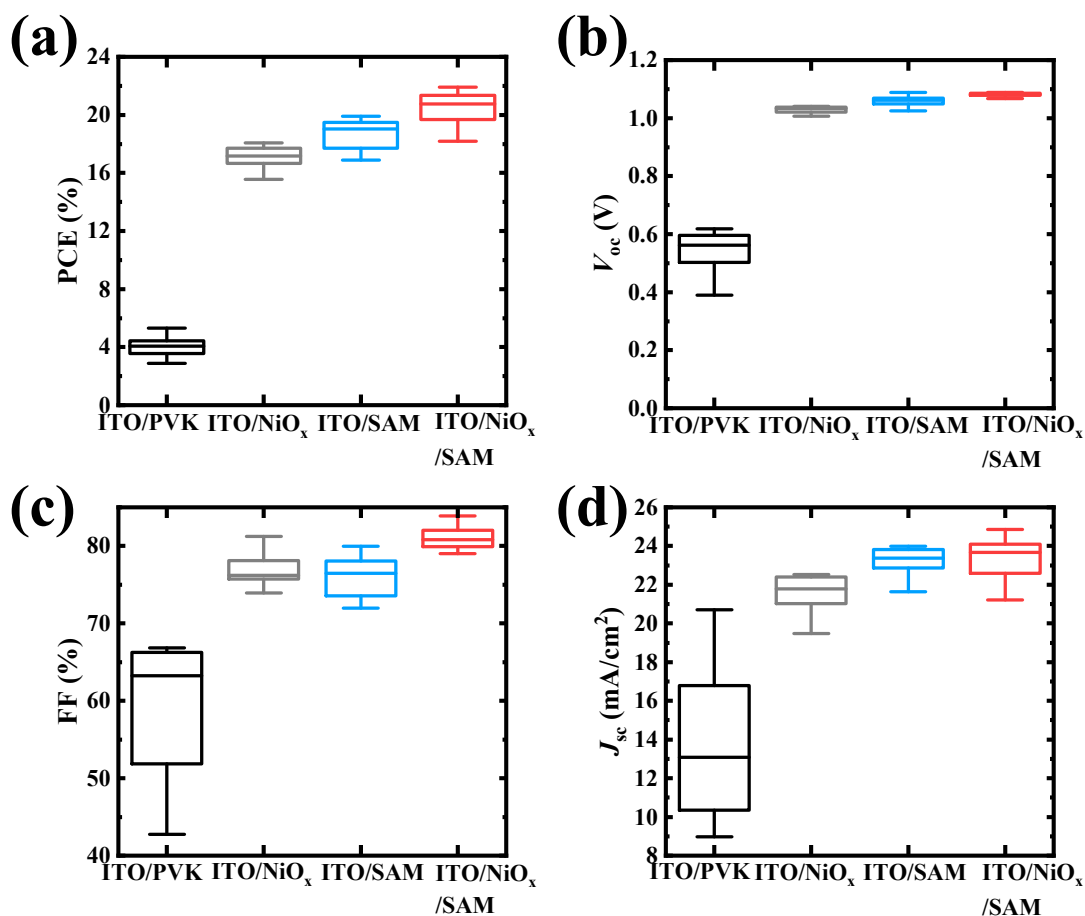


Fig. S11 The box charts of (a) PCE, (b) V_{oc} , (c) FF and (d) J_{sc} for the PSCs based on ITO, ITO/SAM, ITO/NiO_x, and ITO/NiO_x/SAM.

Note 1:

The TRPL decay curve follows the dual exponential decay model:²

$$f(t) = A_1 e^{-\frac{t}{\tau_1}} + A_2 e^{-\frac{t}{\tau_2}} + B$$

$$\tau_{ave} = \frac{A_1 \tau_1^2 + A_2 \tau_2^2}{A_1 \tau_1 + A_2 \tau_2}$$

Where τ_1 is the short transient lifetime, τ_2 is the long transient lifetime, τ_{ave} is the average lifetime, A_1 , A_2 and B are constants.

Table S1. The parameters of TRPL measurement for perovskite films.

Sample	A_1	τ_1 (ns)	A_2	τ_2 (ns)	τ_{ave} (ns)
ITO/PVK	0.28	6.6	0.41	243.3	239.0
ITO/NiO _x /PVK	0.43	4.4	0.25	143.8	136.8
ITO/SAM/PVK	0.39	5.1	0.32	132.3	126.6
ITO/NiO _x /SAM/PVK	0.59	4.8	0.19	103.9	91.5

Note 2:

The dark J-V curves of the “hole-only” devices can be divided into three parts: Ohmic region, trap-filling limited region with a sharp and the trap-free Child’s region. The trap-state density (N_t) of perovskite films is calculated by the equation:^{2, 3}

$$N_t = \frac{2V_{TFL} \varepsilon_0 \varepsilon_r}{eL^2}$$

Where e , ε_0 , ε_r , L and V_{TFL} correspond to the electron charge, vacuum permittivity, relative dielectric constant of perovskite, thickness of perovskite film, and trap-filling limited voltage, respectively. The relative dielectric constant (ε_r) of perovskite was estimated based on existing literature,^{4, 5} and the thickness (L) of perovskite was obtained from cross-sectional SEM.

Note 3:

The band gap calculation of semiconductor materials is based on the following formula:⁶

$$(\alpha h\nu)^{\frac{1}{m}} = B(h\nu - E_g)$$

Where α , h , ν and E_g correspond to absorption coefficient, Planck constant, photon frequency and band gap. Here, for direct bandgap semiconductors, m is equal to 1/2; for indirect bandgap semiconductor materials, m is equal to 2. According to the literature, both NiO_x and perovskite have direct bandgap, while MeO-2PACz has indirect bandgap.⁷

Reference

1. T. Guo, Z. Fang, Z. Zhang, Z. Deng, R. Zhao, J. Zhang, M. Shang, X. Liu, Z. Hu, Y. Zhu and L. Han, *Journal of Energy Chemistry*, 2022, **69**, 211-220.
2. L. Xie, J. Liu, J. Li, C. Liu, Z. Pu, P. Xu, Y. Wang, Y. Meng, M. Yang and Z. Ge, *Advanced Materials*, 2023, **n/a**, 2302752.
3. J. Wang, S. Fu, L. Huang, Y. Lu, X. Liu, J. Zhang, Z. Hu and Y. Zhu, *Advanced Energy Materials*, 2021, **11**, 2102724.
4. R. Su, X. Yang, W. Ji, T. Zhang, L. Zhang, A. Wang, Z. Jiang, Q. Chen, Y. Zhou and B. Song, *Journal of Materials Chemistry C*, 2022, **10**, 18303-18311.
5. J. Zhang, J. Yang, R. Dai, W. Sheng, Y. Su, Y. Zhong, X. Li, L. Tan and Y. Chen, *Advanced Energy Materials*, 2022, **12**, 2103674.
6. K. Ramasamy, H. Sims, W. H. Butler and A. Gupta, *Journal of the American Chemical Society*, 2014, **136**, 1587-1598.
7. J. Sun, C. Shou, J. Sun, X. Wang, Z. Yang, Y. Chen, J. Wu, W. Yang, H. Long, Z. Ying, X. Yang, J. Sheng, B. Yan and J. Ye, *Solar RRL*, 2021, **5**, 2100663.